# Discovery of biased orientation of human DNA motif sequences affecting enhancer-promoter interactions and transcription of genes

Naoki Osato[1*]

[1]Department of Bioinformatic Engineering, Graduate School of Information Science and Technology, Osaka University, Osaka 565-0871, Japan

[*]Corresponding author

E-mail address: naokiosato11@gmail.com, nosato@ist.osaka-u.ac.jp

## Abstract

Chromatin interactions have important roles for enhancer-promoter interactions (EPI) and regulating the transcription of genes. CTCF and cohesin proteins are located at the anchors of chromatin interactions, forming their loop structures. CTCF has insulator function limiting the activity of enhancers into the loops. DNA binding sequences of CTCF indicate their orientation bias at chromatin interaction anchors – forward-reverse (FR) orientation is frequently observed. DNA binding sequences of CTCF were found in open chromatin regions at about 40% - 80% of chromatin interaction anchors in Hi-C and in situ Hi-C experimental data. It has been reported that long range of chromatin interactions tends to include less CTCF at their anchors. It is still unclear what proteins are associated with chromatin interactions.

To find DNA binding motif sequences of transcription factors (TF) such as CTCF affecting the interaction between enhancers and promoters of transcriptional target genes and their expression, here, I predicted human transcriptional target genes of TF bound in open chromatin regions in enhancers and promoters in monocytes and other cell types using experimental data in public database. Transcriptional target genes were predicted based on enhancer-promoter association (EPA). EPA was shortened at the genomic locations of FR orientation of DNA binding motifs of TF, which were supposed to be at chromatin interaction anchors.

The expression level of the target genes predicted based on EPA was compared with target genes predicted from only promoters. Total 351 biased orientation of DNA motifs [192 forward-reverse (FR) and 179 reverse-forward (RF) orientation, the reverse

complement sequences of some DNA motifs are also registered in databases, so the total number is smaller than the number of FR and RF] affected the expression level of putative transcriptional target genes significantly in $CD14^+$ monocytes of four people in common. The same analysis was conducted in $CD4^+$ T cells of four people. DNA motif sequences of CTCF, cohesin and other transcription factors involved in chromatin interactions were found to be biased orientation. Transposon sequences, which are known to be involved in insulators and enhancers, showed biased orientation. Moreover, EPI predicted using FR or RF orientation of DNA motif sequences were overlapped with chromatin interaction data (Hi-C and HiChIP) more than other EPA.

**Keywords:** transcriptional target genes, gene expression, transcription factors, enhancer, enhancer-promoter interactions, chromatin interactions, CTCF, cohesin, open chromatin regions

## Background

Chromatin interactions have important roles for enhancer-promoter interactions (EPI) and regulating the transcription of genes. CTCF and cohesin proteins are located at the anchors of chromatin interactions, forming their loop structures. CTCF has insulator function limiting the activity of enhancers into the loops (Fig. 1A). DNA binding sequences of CTCF indicate their orientation bias at chromatin interaction anchors – forward-reverse (FR) orientation is frequently observed (de Wit et al. 2015; Guo et al. 2015). About 40% - 80% of chromatin interaction anchors of Hi-C and in situ

55 Hi-C experiments include DNA binding motif sequences of CTCF. However, it has been
56 reported that long range of chromatin interactions tends to include less CTCF at their
57 anchors (Jeong et al. 2017). Other DNA binding proteins such as ZNF143, YY1, and
58 SMARCA4 (BRG1) are found to be associated with chromatin interactions and EPI
59 (Bailey et al. 2015; Barutcu et al. 2016; Weintraub et al. 2017). CTCF, cohesin, ZNF143,
60 YY1 and SMARCA4 have other biological functions as well as chromatin interactions
61 and enhancer-promoter interactions. The DNA binding motif sequences of the
62 transcription factors are found in open chromatin regions near transcriptional start sites
63 (TSS) as well as chromatin interaction anchors.

64 DNA binding motif sequence of ZNF143 was enriched at both chromatin
65 interaction anchors. ZNF143's correlation with the CTCF-cohesin cluster relies on its
66 weakest binding sites, found primarily at distal regulatory elements defined by the
67 'CTCF-rich' chromatin state. The strongest ZNF143-binding sites map to promoters
68 bound by RNA polymerase II (POL2) and other promoter-associated factors, such as the
69 TATA-binding protein (TBP) and the TBP-associated protein, together forming a
70 'promoter' cluster (Bailey et al. 2015).

71 DNA binding motif sequence of YY1 does not seem to be enriched at both
72 chromatin interaction anchors (Z-score < 2), whereas DNA binding motif sequence of
73 ZNF143 is significantly enriched (Z-score > 7; Bailey et al. 2015 Figure 2a). In the
74 analysis of YY1, to identify a protein factor that might contribute to EPI, (Ji et al. 2015)
75 performed chromatin immune precipitation with mass spectrometry (ChIP-MS), using
76 antibodies directed toward histones with modifications characteristic of enhancer and

77 promoter chromatin (H3K27ac and H3K4me3, respectively). Of 26 transcription factors
78 that occupy both enhancers and promoters, four are essential based on a CRISPR
79 cell-essentiality screen and two (CTCF, YY1) are expressed in >90% of tissues
80 examined (Weintraub et al. 2017). These analyses started from the analysis of histone
81 modifications of an enhancer mark rather than chromatin interactions. Other protein
82 factors associated with chromatin interactions may be found from other researches.

83 As computational approaches, machine-learning analyses to predict chromatin
84 interactions have been proposed (Schreiber et al. 2017; Zhang et al. 2017). However,
85 they were not intended to find DNA motif sequences of transcription factors affecting
86 chromatin interactions, EPI, and the expression level of transcriptional target genes,
87 which were examined in this study.

88 DNA binding proteins involved in chromatin interactions are supposed to affect
89 the transcription of genes in the loop formed by chromatin interactions. In my previous
90 analyses, the expression level of human putative transcriptional target genes was
91 affected, according to the criteria of enhancer-promoter association (EPA) (Fig. 1B;
92 (Osato 2018)). EPI predicted based on EPA shortened at the genomic locations of
93 forward-reverse orientation of CTCF binding sites affected the expression level of
94 putative transcriptional target genes the most, compared with the expression level of
95 transcriptional target genes predicted from only promoters (Fig. 1B). The expression
96 level tended to be increased in monocytes and $CD4^+$ T cells, implying that enhancers
97 activated the transcription of genes, and decreased in ES and iPS cells, implying that
98 enhancers repressed the transcription of genes. These analyses suggested that enhancers

99 affected the transcription of genes significantly, when EPI were predicted properly.
100 Other DNA binding proteins involved in chromatin interactions, as well as CTCF,
101 would locate at chromatin interaction anchors with a pair of biased orientation of DNA
102 binding motif sequences, affecting the expression level of putative transcriptional target
103 genes in the loop formed by the chromatin interactions. As experimental issues of the
104 analyses of chromatin interactions, chromatin interaction data are changed, according to
105 experimental techniques, depth of DNA sequencing, and even replication sets of the
106 same cell type. Chromatin interaction data may not be saturated enough to cover all
107 chromatin interactions. Supposing these characters of DNA binding proteins associated
108 with chromatin interactions and avoiding experimental issues of the analyses of
109 chromatin interactions, here I searched for DNA motif sequences of transcription factors
110 and repeat DNA sequences, affecting EPI and the expression level of putative
111 transcriptional target genes in $CD14^+$ monocytes and $CD4^+$ T cells of four people and
112 other cell types without using chromatin interaction data. Then, putative EPI were
113 compared with chromatin interaction data.
114

115 ## Results

116 **Search for biased orientation of DNA motif sequences**

117 Transcription factor binding sites (TFBS) were predicted using open chromatin
118 regions and DNA motif sequences of transcription factors collected from various
119 databases and journal papers (see Methods). Transcriptional target genes were predicted
120 using TFBS in promoters and enhancer-promoter association (EPA) shortened at the

121 genomic locations of DNA binding motif sequences of transcription factors such as
122 CTCF and cohesins (RAD21 and SMC3). To find DNA motif sequences of transcription
123 factors, other than CTCF and cohesin, and repeat DNA sequences affecting the
124 expression level of putative transcriptional target genes, transcriptional target genes of
125 each transcription factor were predicted based on EPA shortened at the genomic
126 locations of DNA motif sequences, and the expression level of the putative
127 transcriptional target genes was compared with those predicted from promoters using
128 Mann Whiteney U test ($p$-value < 0.05). The number of transcription factors showing a
129 significant difference of expression level of putative transcriptional target genes was
130 counted. To examine whether the orientation of DNA motif sequences shortening EPA
131 affected the number of transcription factors showing a significant difference of
132 expression level of putative transcriptional target genes, the number of the transcription
133 factors was compared among forward-reverse, reverse-forward, and any orientation of
134 DNA motif sequences shortening EPA, using chi-square test ($p$-value < 0.05). To avoid
135 missing DNA motif sequences showing a relatively weak statistical significance by
136 multiple testing collection, the above analyses were conducted using monocytes of four
137 people independently, and DNA motif sequences found in monocytes of four people in
138 common were selected. Total 351 of biased (192 forward-reverse and 179
139 reverse-forward) orientation of DNA binding motif sequences of transcription factors
140 have been found in monocytes of four people in common, whereas only one any
141 orientation (i.e. without considering orientation) of DNA binding motif sequences have
142 been found in monocytes of four people in common (Fig. 2; Table 1; Supplemental

143 Table S1). Forward-reverse orientation of DNA motif sequences included CTCF,
144 cohesin (RAD21 and SMC3), ZNF143 and YY1, which are associated with chromatin
145 interactions and enhancer-promoter interactions (EPI). SMARCA4 (BRG1) is
146 associated with topologically associated domain (TAD), which is higher-order
147 chromatin organization. The DNA binding motif sequences of SMARCA4 was not
148 registered in the databases used in this study. Forward-reverse orientation of DNA motif
149 sequences included SMRC2, a member of the same SWI/SNF family of proteins as
150 SMARCA4.

151 The same analysis was conducted using DNase-seq data of $CD4^+$ T cells of four
152 people. Total 322 of biased (186 forward-reverse and 166 reverse-forward) orientation
153 of DNA binding motif sequences of transcription factors have been found in T cells of
154 four people in common, whereas only five any orientation (i.e. without considering
155 orientation) of DNA binding motif sequences have been found in T cells of four people
156 in common (Supplemental Table S2). Biased orientation of DNA motif sequences in T
157 cells included CTCF, cohesion (RAD21 and SMC3), YY1, and SMARC. Biased
158 orientation of DNA motif sequences in T cells included JUNDM2 (JDP2), which is
159 involved in histone-chaperone activity, promoting nucleosome, and inhibition of histone
160 acetylation (Jin et al. 2006). JDP2 forms a homodimer or heterodimer with various
161 transcription factors (https://en.wikipedia.org/wiki/Jun_dimerization_protein). Among
162 322, 53 of biased orientation of DNA binding motif sequences of transcription factors
163 were found in both monocytes and T cells in common (Supplemental Table S3). For
164 each orientation, 27 forward-reverse and 29 reverse-forward orientation of DNA

165 binding motif sequences of transcription factors were found in both monocytes and T
166 cells in common. Without considering the difference of orientation of DNA binding
167 motif sequences, 79 of biased orientation of DNA binding motif sequences of
168 transcription factors were found in both monocytes and T cells. As a reason for the
169 increase of the number from 53, a transcription factor or an isoform of the same
170 transcription factor may bind to a different DNA binding motif sequence according to
171 cell types. The same transcription factor has several DNA binding motif sequences and
172 in some cases one of the motif sequence is almost the same as the reverse complement
173 sequence of another motif sequence of the same transcription factor. I reported that a
174 complex of transcription factors binds to a slightly different DNA binding motif
175 sequence from the combination of DNA binding motif sequences of transcription factors
176 consisting of the complex in *C. elegans* (Tabuchi et al. 2011). From another viewpoint
177 of this study, the expression level of putative transcription target genes of some
178 transcription factors would be different, depending on the genomic locations (enhancers
179 or promoters) of DNA binding motif sequences of the transcription factors in monocytes
180 and T cells of four people.

181 To examine whether the biased orientation of DNA binding motif sequences of
182 transcription factors was observed in other cell types, the same analyses were conducted
183 in other cell types. However, for other cell types, experimental data of one sample were
184 available in ENCODE database, so the analyses of DNA motif sequences were
185 performed by comparing with the result in monocytes of four people. Among the biased
186 orientation of DNA binding motif sequences found in monocytes, 79, 76, 91, 61, and 59

187 DNA binding motif sequences were also observed in $CD4^+$ T cells, H1-hESC, iPS,
188 Huvec and MCF-7 respectively, including CTCF and cohesin (RAD21 and SMC3)
189 (Table 2; Supplemental Table S4). The scores of DNA binding motif sequences were the
190 highest in monocytes, and the other cell types showed lower scores. The results of the
191 analysis of DNA motif sequences in $CD20^+$ B cells and macrophages did not include
192 CTCF and cohesin, because these analyses can be utilized in cells where the expression
193 level of putative transcriptional target genes of each transcription factor show a
194 significant difference between promoters and EPA shortened at the genomic locations of
195 DNA motif sequences. Some experimental data of a cell did not show a significant
196 difference between promoters and EPA (Osato 2018).

197 Instead of DNA binding motif sequences of transcription factors, repeat DNA
198 sequences were also examined. The expression level of transcriptional target genes
199 predicted based on EPA shortened at the genomic locations of repeat DNA sequences
200 was compared with the expression level of transcriptional target genes predicted from
201 promoters. Three reverse-forward orientation of repeat DNA sequences showed a
202 significant difference of expression level of putative transcriptional target genes in
203 monocytes of four people in common (Table 3). Among them, LTR16C repeat DNA
204 sequence was observed in iPS and H1-hESC. The same as $CD14^+$ monocytes, biased
205 orientation of repeat DNA sequences was examined in $CD4^+$ T cells. Three
206 forward-reverse and two reverse-forward orientation of repeat DNA sequences showed
207 a significant difference of expression level of putative transcriptional target genes in T
208 cells of four people in common (Supplemental Table S5) Among them, MIRb repeat

209 DNA sequence was observed in monocytes, and MIR3 was observed in monocytes and
210 huvec. MIR and other transposon sequences are known to be involved in insulators and
211 enhancers (Bejerano et al. 2006; Rebollo et al. 2012; de Souza et al. 2013; Jjingo et al.
212 2014; Wang et al. 2015).
213
214 **Co-location of biased orientation of DNA motif sequences**
215 To examine association of 351 biased (forward-reverse and reverse-forward)
216 orientation of DNA binding motif sequences of transcription factors, co-location of the
217 DNA binding motif sequences in open chromatin regions in monocytes was analyzed.
218 The number of open chromatin regions with the same pairs of DNA binding motif
219 sequences was counted, and when the pairs of DNA binding motif sequences were
220 enriched with statistical significance (chi-square test, $p$-value $< 1.0 \times 10^{-10}$), they were
221 listed (Table 4; Supplemental Table S6). Open chromatin regions overlapped with
222 histone modification of an enhancer mark (H3K27ac) (total 26,095 regions) showed a
223 larger number of enriched pairs of DNA motifs than all open chromatin regions (Table
224 4; Supplemental Table S6). H3K27ac is known to be enriched at chromatin interaction
225 anchors (Phanstiel et al. 2017). As already known, CTCF was found with cohesin such
226 as RAD21 and SMC3 (Table 4). Top 30 pairs of FR and RF orientations of DNA motifs
227 co-occupied in the same open chromatin regions were shown (Table 4). Total number of
228 pairs of DNA motifs was 569, consisting of 137 unique DNA motifs, when the pair of
229 DNA motifs were observed in more than 80% of the number of open chromatin regions
230 with the DNA motifs.

231 The same as $CD14^+$ monocytes, to examine association of 322 biased orientation
232 of DNA binding motif sequences of transcription factors, co-location of the DNA
233 binding motif sequences in open chromatin regions in $CD4^+$ T cells was analyzed. Top
234 30 pairs of FR and RF orientations of DNA motifs co-occupied in the same open
235 chromatin regions were shown (Supplemental Table S7). Total number of pairs of DNA
236 motifs was 156, consisting of 77 unique DNA motifs, when the pair of DNA motifs
237 were observed in more than 60% of the number of open chromatin regions with the
238 DNA motifs (chi-square test, $p$-value $< 1.0 \times 10^{-10}$). Thought the number of biased
239 orientation of DNA motif sequences was similar between monocytes and T cell, and the
240 number of biased orientation of repeat DNA sequences was larger in T cells, the number
241 of pairs of DNA motifs in T cells was much smaller than monocytes. This result was
242 obtained from the analysis of DNase-seq and H3K27ac ChIP-seq data of a donor (SRA
243 database: SRR097566), but the analyses of other donors also showed the same tendency.
244 Four pairs of DNA motif sequences including a pair of CTCF and SMC3 in T cells were
245 found in monocytes in common (Supplemental Table S7). Though the list of biased
246 orientation of DNA motif sequences of transcription factors in T cells included RAD21,
247 it was not significantly co-localized with other DNA motif sequences in T cells under
248 the search condition.
249
250 **Comparison with chromatin interaction data**
251 To examine whether the biased orientation of DNA motif sequences is associated
252 with chromatin interactions, enhancer-promoter interactions (EPI) predicted based on

253 enhancer-promoter associations (EPA) were compared with chromatin interaction data
254 (Hi-C). Due to the resolution of Hi-C experimental data used in this study (50kb), EPI
255 were adjusted to 50kb resolution. EPI were predicted based on three types of EPA: (i)
256 EPA without being shortened by DNA motif sequences, (ii) EPA shortened at the
257 genomic locations of DNA motif sequences of transcription factors such as CTCF and
258 cohesin (RAD21, SMC3) without considering their orientation, and (iii) EPA shortened
259 at the genomic locations of forward-reverse or reverse-forward orientation of DNA
260 motif sequences of transcription factors. EPA (iii) showed the highest ratio of EPI
261 overlapped with chromatin interactions (Hi-C) using DNA binding motif sequences of
262 CTCF and cohesin (RAD21 and SMC3), compared with the other two types of EPA
263 (Fig. 3). Total 62 biased orientation (41 FR and 24 RF) of DNA motif sequences
264 including CTCF and cohesin showed a higher ratio of EPI overlapped with Hi-C than
265 the other types of EPA in monocytes (Table 5). Chromatin interaction data were
266 obtained using different samples from DNase-seq, open chromatin regions, so
267 individual differences seemed to be large from the results of this analysis. Since, for
268 some DNA motif sequences of transcription factors, the number of EPI overlapped with
269 chromatin interactions was small, if higher resolution of chromatin interaction data
270 (such as HiChIP, in situ DNase Hi-C, and in situ Hi-C data, or a tool to improve the
271 resolution such as HiCPlus) is available, the number of EPI overlapped with chromatin
272 interactions would be increased and the difference of the numbers among three types of
273 EPA might be larger and more significant than the current results (Rao et al. 2014;
274 Ramani et al. 2016; Mumbach et al. 2017; Zhang et al. 2018).

275 After the analysis of $CD14^+$ monocytes, to utilize HiChIP chromatin interaction
276 data in $CD4^+$ T cells, the same analysis for $CD14^+$ monocytes was performed using
277 DNase-seq data of four donors in $CD4^+$ T cells (Mumbach et al. 2017). EPI predicted
278 based on EPA were compared with HiChIP chromatin interaction data in $CD4^+$ T cells.
279 The resolutions of HiChIP chromatin interaction data and EPI were adjusted to 1kb. EPI
280 were predicted based on the three types of EPA in the same way as $CD14^+$ monocytes.
281 EPA (iii) showed the highest ratio of EPI overlapped with chromatin interactions
282 (HiChIP) using DNA binding motif sequences of CTCF and cohesin (RAD21 and
283 SMC3), compared with the other two types of EPA (Supplemental Fig. S2). Total 150
284 biased orientation (92 FR and 66 RF) of DNA motif sequences including CTCF and
285 cohesin showed a higher ratio of EPI overlapped with HiChIP than the other types of
286 EPA in monocytes (Supplemental Table S8). As expected, the number of EPI
287 overlapped with chromatin interactions (HiChIP) was increased, compared with Hi-C
288 chromatin interactions. However, the same as $CD14^+$ monocytes, chromatin interaction
289 data were obtained using different samples from DNase-seq, open chromatin regions in
290 $CD4^+$ T cells, so individual differences seemed to be large from the results of this
291 analysis, and (Mumbach et al. 2017) suggested that individual differences of chromatin
292 interactions were larger than those of open chromatin regions. ATAC-seq data, open
293 chromatin regions were available in $CD4^+$ T cells in the paper, however, when using
294 ATAC-seq data, the result of the analysis of biased orientation of DNA motif sequences
295 was different from DNase-seq data, and not included a part of CTCF and cohesin. Thus,
296 DNase-seq data collected from ENCODE and Blueprint projects were employed in this

297 study.

298

299 **Discussion**

300 To find DNA motif sequences of transcription factors and repeat DNA sequences
301 affecting human putative transcriptional target genes, DNA motif sequences were
302 searched from open chromatin regions of monocytes of four people. Total 351 biased
303 (192 forward-reverse and 179 reverse-forward) orientation of DNA motif sequences
304 were found in monocytes of four people in common, whereas only one any orientation
305 (i.e. without considering orientation) of DNA motif sequence was found to affect
306 putative transcriptional target genes, suggesting that EPA shortened at the genomic
307 locations of forward-reverse or reverse-forward orientation of DNA motif sequences of
308 transcription factors is an important character for EPI and transcription of genes.

309 When DNA motif sequences were searched from monocytes of one person, a
310 larger number of biased orientation of DNA motif sequences affecting human putative
311 transcriptional target genes has been found. When the number of people, from which
312 experimental data were obtained, was increased, the number of DNA motif sequences
313 found in all people in common decreased and in some cases, known transcription
314 factors involved in chromatin interactions such as CTCF and cohesin (RAD21 and
315 SMC3) were not identified by statistical tests. This would be caused by individual
316 difference of the same cell type, low quality of experimental data, and experimental
317 errors. Moreover, though forward-reverse orientation of DNA binding motif sequences
318 of CTCF and cohesin is frequently observed at chromatin interaction anchors, the

319 percentage of forward-reverse orientation is not 100, and other orientations of the DNA
320 binding motif sequences are also observed. Though DNA binding motif sequences of
321 CTCF and cohesin are found in various open chromatin regions, DNA binding motif
322 sequences of some transcription factors would be observed less frequently in open
323 chromatin regions. The analyses of cells of a number of people would avoid missing
324 relatively weak statistical significance of DNA motif sequences in cells of each person
325 by multiple testing correction of thousands of statistical tests. A DNA motif sequence
326 was found with $p$-value < 0.05 in cells of one person and the DNA motif sequence
327 found in the same cell type of four people in common would have $p$-value < $(0.05)^4$ =
328 0.00000625. Actually, DNA motif sequences with $p$-value slightly less than 0.05 in
329 monocytes of one person were observed in monocytes of four people in common.

330 EPI were compared with chromatin interactions (Hi-C) in monocytes. EPA
331 shortened at the genomic locations of DNA binding motif sequences of CTCF and
332 cohesin (RAD21 and SMC3) showed a significant difference of the ratios of EPI
333 overlapped with chromatin interactions, according to three types of EPA (FR, any, and
334 others). Using open chromatin regions overlapped with ChIP-seq experimental data of
335 histone modification of an enhancer mark (H3K27ac), the ratio of EPI not overlapped
336 with Hi-C was reduced and the difference of the ratio of EPI overlapped with chromatin
337 interactions among the three types of EPA became larger (data not shown). (Phanstiel et
338 al. 2017) also reported that there was an especially strong enrichment for loops with
339 H3K27 acetylation peaks at both ends (Fisher's Exact Test, $p = 1.4 \times 10^{-27}$). However,
340 the total number of EPI overlapped with chromatin interactions was also reduced using

341 H3K27ac peaks, so more chromatin interaction data would be needed to obtain reliable
342 results in this study. As an issue of experimental data, chromatin interaction data were
343 obtained using different samples from DNase-seq, open chromatin regions, so
344 individual differences were not reflected to chromatin interaction data. Moreover, the
345 resolution of chromatin interaction data used in monocytes is about 50kb, thus the
346 number of chromatin interactions was relatively small (72,284 at 50kb resolution with
347 cutoff score of CHiCAGO tool > 1). EPA shortened at the genomic locations of DNA
348 binding motif sequences of transcription factors found in various open chromatin
349 regions such as CTCF and cohesin (RAD21 and SMC3) tend to be overlapped with a
350 larger number of chromatin interactions than DNA binding motif sequences of
351 transcription factors less frequently observed in open chromatin regions. Therefore, to
352 examine the difference of the numbers of EPI overlapped with chromatin interactions,
353 according to three types of EPA (FR or RF, any, and others), the number of chromatin
354 interactions should be large enough.

355 As HiChIP chromatin interaction data were available in $CD4^+$ T cells, biased
356 orientations of DNA motif sequences of transcription factors were examined in T cells
357 using DNase-seq data of four people. The resolutions of chromatin interactions and EPI
358 were adjusted to 1kb by fragmentation of genome sequences. In monocytes, the
359 resolution of Hi-C chromatin interaction data was converted by extending anchor
360 regions of chromatin interactions to 50kb length and merging chromatin interactions
361 overlapped with each other. Fragmentation of genome sequences may affect the
362 classification of chromatin interactions of which anchors are located near the border of a

363 fragment, but the number of chromatin interactions would not be decreased, compared
364 with merging chromatin interactions. The number of HiChIP chromatin interactions was
365 28,918,687 at 1kb resolution. As expected, the number of EPI overlapped with
366 chromatin interactions was increased, and about half of biased orientation of DNA motif
367 sequences of transcription factors showed a statistical significance in EPI predicted
368 based on EPA shortened at the genomic locations of the DNA motif sequences,
369 compared with the other types of EPA. But the difference of the ratios of EPI
370 overlapped with chromatin interactions, according to three types of EPA (FR or RF, any,
371 and others), became smaller in T cells than monocytes (Supplemental Fig. S2), due to
372 the increase of chromatin interactions. False positive predictions of EPI would be
373 decreased by using H3K27ac marks and other features, as suggested in the analysis in
374 monocytes.

375 Though the number of known DNA binding proteins and transcription factors
376 involved in chromatin interactions would be less than 20 or so, about 300 DNA binding
377 proteins showed enrichment of biased orientation of their DNA binding sequences, and
378 known DNA binding proteins involved in chromatin interactions were found in the
379 biased orientation of DNA binding sequences. JUNDM2 (JDP2) found in T cells is not
380 known DNA binding proteins involved in chromatin interactions. JDP2 is involved in
381 histone and nucleosome-related functions such as histone-chaperone activity, promoting
382 nucleosome, and inhibition of histone acetylation (Jin et al. 2006). JDP2 forms a
383 homodimer or heterodimer with various transcription factors
384 (https://en.wikipedia.org/wiki/Jun_dimerization_protein). Thus, the main function of

385 JDP2 may not be associated with chromatin interactions, but it forms a homodimer or
386 heterodimer with transcription factors, potentially forming a chromatin interaction
387 through the binding of JDP2 and another transcription factor, like chromatin interactions
388 formed by YY1 transcription factor (Weintraub et al. 2017). When forming a
389 homodimer or heterodimer with another transcription factor, transcription factors may
390 bind to genome DNA with a specific orientation of their DNA binding sequences. From
391 the analysis of biased orientation of DNA motif sequences of transcription factors, such
392 transcription factors would also be found. If the DNA binding motif sequence of only
393 the mate to a pair of transcription factors was found in EPA, EPA was shortened at one
394 side, the genomic location of the DNA binding motif sequence of the mate to the pair,
395 and transcriptional target genes were predicted using the EPA shortened at one side. In
396 this analysis, the mate to both heterodimer and homodimer of transcription factors can
397 be used to examine the effect on the expression level of transcriptional target genes
398 predicted based on the EPA shortened at one side.

399 I reported that the ratio of the number of functional enrichment of putative
400 transcriptional target genes in the total number putative transcriptional target genes
401 changed according to the types of EPA, in the same way as gene expression level (Osato
402 2018). JDP2 showed a higher ratio of functional enrichment of putative transcriptional
403 target genes using EPA shortened at genomic locations of forward-reverse orientation of
404 the DNA binding motif sequence, compared with the other types of EPA
405 (reverse-forward or any orientation) in monocytes and T cells, among monocytes, T
406 cells and $CD20^+$ B cells. While the genome-wide analysis of functional enrichments of

407 putative transcriptional target genes takes computational time, the genome-wide
408 analysis of gene expression level is finished with less computational time. The analysis
409 of gene expression level can be used for a cell type and experimental data where the
410 expression levels of transcriptional target genes predicted from EPA are significantly
411 different from those predicted from only promoter.

412 The analyses in this study revealed novel characters of DNA binding motif
413 sequences of transcription factors and repeat DNA sequences, and would be useful to
414 analyze transcription factors involved in chromatin interactions and/or forming a
415 homodimer, heterodimer or complex with other transcription factors, affecting the
416 expression and transcriptional regulation of genes.

417

418 ## Methods

419 **Search for biased orientation of DNA motif sequences**

420 To examine transcriptional regulatory target genes, bed files of hg38 of Blueprint
421 DNase-seq data for $CD14^+$ monocytes of four donors (EGAD00001002286; Donor ID:
422 C0010K, C0011I, C001UY, C005PS) were obtained from Blueprint project web site
423 (http://dcc.blueprint-epigenome.eu/#/home), and the bed files of hg38 were converted
424 into those of hg19 using Batch Coordinate Conversion (liftOver) web site
425 (https://genome.ucsc.edu/util.html). Bed files of hg19 of ENCODE
426 $CD4^+$_Naive_Wb11970640 (GSM1014537; UCSC Accession: wgEncodeEH003156),
427 H1-hESC (GSM816632; UCSC Accession: wgEncodeEH000556), iPSC (GSM816642;
428 UCSC Accession: wgEncodeEH001110), HUVEC (GSM1014528; UCSC Accession:

429 wgEncodeEH002460), and MCF-7 (GSM816627; UCSC Accession:
430 wgEncodeEH000579) were obtained from the ENCODE websites
431 (http://hgdownload.cse.ucsc.edu/goldenPath/hg19/encodeDCC/wgEncodeUwDgf/;
432 http://hgdownload.cse.ucsc.edu/goldenPath/hg19/encodeDCC/wgEncodeUwDnase/).
433 As high resolution of chromatin interaction data using HiChIP became available
434 in $CD4^+$ T cells, to promote the same analysis of $CD14^+$ monocytes in $CD4^+$ T cells,
435 DNase-seq data of four donors were obtained from ENCODE and Blueprint projects
436 web sites. DNase-seq data of only one donor was available in Blueprint project for
437 $CD4^+$ T cells (Donor ID: S008H1), and three other DNase-seq data were obtained from
438 ENCODE project. Though the peak calling of DNase-seq data available in ENCODE
439 database was different from other DNase-seq data in ENCODE and Blueprint projects
440 where 150bp length of peaks were usually predicted using HotSpot (John et al. 2011),
441 FASTQ files of DNase-seq data were downloaded from NCBI Sequence Read Archive
442 (SRA) database (SRR097566, SRR097618, and SRR171574). Read sequences of
443 FASTQ files were aligned to the hg19 version of the human genome reference using
444 BWA (Li and Durbin 2009), and the BAM files generated by BWA were converted into
445 SAM files, sorted, and indexed using Samtools (Li et al. 2009). Peaks of the DNase-seq
446 data were predicted using HotSpot-4.1.1.
447 To identify transcription factor binding sites (TFBS) from the DNase-seq data,
448 TRANSFAC (2013.2), JASPAR (2010), UniPROBE, BEEML-PBM, high-throughput
449 SELEX, Human Protein-DNA Interactome, and transcription factor binding sequences
450 of ENCODE ChIP-seq data were used (Wingender et al. 1996; Newburger and Bulyk

451 2009; Portales-Casamar et al. 2010; Xie et al. 2010; Zhao and Stormo 2011; Jolma et al.
452 2013; Kheradpour and Kellis 2014). Position weight matrices of transcription factor
453 binding sequences were transformed into TRANSFAC matrices and then into MEME
454 matrices using in-house scripts and transfac2meme in MEME suite (Bailey et al. 2009).
455 Transcription factor binding sequences of transcription factors derived from vertebrates
456 were used for further analyses. Searches were conducted for transcription factor binding
457 sequences from each narrow peak using FIMO with *p*-value threshold of $10^{-5}$ (Grant et
458 al. 2011). Transcription factors corresponding to transcription factor binding sequences
459 were searched computationally by comparing their names and gene symbols of HGNC
460 (HUGO Gene Nomenclature Committee) -approved gene nomenclature and 31,848
461 UCSC known canonical transcripts
462 (http://hgdownload.cse.ucsc.edu/goldenpath/hg19/database/knownCanonical.txt.gz), as
463 transcription factor binding sequences were not linked to transcript IDs such as UCSC,
464 RefSeq, and Ensembl transcripts.

465 Target genes of a transcription factor were assigned when its TFBS was found in
466 DNase-seq narrow peaks in promoter or extended regions for enhancer-promoter
467 association of genes (EPA). Promoter and extended regions were defined as follows:
468 promoter regions were those that were within distances of ±5 kb from transcriptional
469 start sites (TSS). Promoter and extended regions were defined as per the following
470 association rule, which is the same as that defined in Figure 3A of a previous study
471 (McLean et al. 2010): the single nearest gene association rule, which extends the
472 regulatory domain to the midpoint between the TSS of the gene and that of the nearest

473 gene upstream and downstream without the limitation of extension length. Extended
474 regions for EPA were shortened at the genomic locations of DNA binding sites of
475 transcription factors that were the closest to a transcriptional start site, and
476 transcriptional target genes were predicted from the shortened enhancer regions using
477 TFBS. Furthermore, promoter and extended regions for EPA were shortened at the
478 genomic locations of forward–reverse orientation of DNA binding sites of transcription
479 factors. When forward or reverse orientation of DNA binding sites were continuously
480 located in genome sequences several times, the most external forward–reverse
481 orientation of DNA binding sites were selected. The genomic positions of genes were
482 identified using 'knownGene.txt.gz' file in UCSC bioinformatics sites (Karolchik et al.
483 2014). The file 'knownCanonical.txt.gz' was also utilized for choosing representative
484 transcripts among various alternate forms for assigning promoter and extended regions
485 for EPA. From the list of transcription factor binding sequences and transcriptional
486 target genes, redundant transcription factor binding sequences were removed by
487 comparing the target genes of a transcription factor binding sequence and its
488 corresponding transcription factor; if identical, one of the transcription factor binding
489 sequences was used. When the number of transcriptional target genes predicted from a
490 transcription factor binding sequence was less than five, the transcription factor binding
491 sequence was omitted.

492 Repeat DNA sequences were searched from the hg19 version of the human
493 reference genome using RepeatMasker (Smit, AFA & Green, P RepeatMasker at
494 http://www.repeatmasker.org) and RepBase RepeatMasker Edition

495 (http://www.girinst.org).

496 For gene expression data, RNA-seq reads mapped onto human hg19 genome
497 sequences were obtained, including ENCODE long RNA-seq reads with poly-A of
498 H1-hESC, iPSC, HUVEC, and MCF-7 (GSM26284, GSM958733, GSM2344099,
499 GSM2344100, GSM958734, and GSM765388), and UCSF-UBC human reference
500 epigenome mapping project RNA-seq reads with poly-A of naive $CD4^+$ T cells
501 (GSM669617). Two replicates were present for H1-hESC, iPSC, HUVEC, and MCF-7,
502 and a single one for $CD4^+$ T cells. RPKMs of the RNA-seq data were calculated using
503 RSeQC (Wang et al. 2012). For monocytes, Blueprint RNA-seq RPKM data
504 (GSE58310, GSE58310_GeneExpression.csv.gz, Monocytes_Day0_RPMI) was used
505 (Saeed et al. 2014). Based on RPKM, UCSC transcripts with expression levels among
506 top 30% of all the transcripts were selected in each cell type.

507 The expression level of transcriptional target genes predicted based on EPA
508 shortened at the genomic locations of DNA motif sequences of transcription factors or
509 repeat DNA sequences was compared with the expression level of transcriptional target
510 genes predicted from promoter. For each DNA motif sequence shortening EPA,
511 transcriptional target genes were predicted using about 3,000 – 5,000 DNA binding
512 motif sequences of transcription factors, and the expression level of putative
513 transcriptional target genes of each transcription factor was compared between EPA and
514 only promoter using Mann-Whitney test ($p$-value $< 0.05$). The number of transcription
515 factors showing a significant difference of expression level of putative transcriptional
516 target genes between EPA and promoter was compared among forward-reverse,

517 reverse-forward, and any orientation of DNA motif sequences shortening EPA using
518 chi-square test ($p$-value < 0.05). When DNA motif sequences of transcription factors or
519 repeat DNA sequences shortening EPA showed a significant difference of expression
520 level of putative transcriptional target genes in forward-reverse, reverse-forward, or any
521 orientation in monocytes of four people in common, the DNA motif sequences were
522 listed.

523 Though forward-reverse orientation of DNA binding motif sequences of CTCF
524 and cohesin is frequently observed at chromatin interaction anchors, the percentage of
525 forward-reverse orientation is not 100, and other orientations of the DNA binding motif
526 sequences are also observed. Though DNA binding motif sequences of CTCF and
527 cohesin are found in various open chromatin regions, DNA binding motif sequences of
528 some transcription factors would be observed less frequently in open chromatin regions.
529 The analyses of cells of a number of people would avoid missing relatively weak
530 statistical significance of DNA motif sequences in cells of each person by multiple
531 testing correction of thousands of statistical tests. A DNA motif sequence was found
532 with $p$-value < 0.05 in cells of one person and the DNA motif sequence found in the
533 same cell type of four people in common would have $p$-value < $0.05^4 = 0.00000625$.

534

535 **Co-location of biased orientation of DNA motif sequences**

536 Co-location of biased orientation of DNA binding motif sequences of
537 transcription factors was examined. The number of open chromatin regions with the
538 same pairs of DNA binding motif sequences was counted, and when the pairs of DNA

539 binding motif sequences were enriched with statistical significance (chi-square test,
540 $p$-value < $1.0 \times 10^{-10}$), they were listed.

541 For histone modification of an enhancer mark (H3K27ac), bed files of hg38 of
542 Blueprint ChIP-seq data for $CD14^+$ monocytes (EGAD00001001179) and $CD4^+$ T cells
543 (Donor ID: S000RD) was obtained from Blueprint web site
544 (http://dcc.blueprint-epigenome.eu/#/home), and the bed files of hg38 were converted
545 into those of hg19 using Batch Coordinate Conversion (liftOver) web site
546 (https://genome.ucsc.edu/util.html).

547

548 **Comparison with chromatin interaction data**

549 For comparison of EPA in monocytes with chromatin interactions,
550 'PCHiC_peak_matrix_cutoff0.txt.gz' file was downloaded from 'Promoter Capture
551 Hi-C in 17 human primary blood cell types' web site (https://osf.io/u8tzp/files/), and
552 chromatin interactions for Monocytes with scores of CHiCAGO tool > 1 were extracted
553 from the file (Javierre et al. 2016).

554 EPI were predicted using three types of EPA in monocytes: (i) EPA shortened at
555 the genomic locations of forward-reverse or reverse-forward orientation of DNA motif
556 sequences of transcription factors, (ii) EPA shortened at the genomic locations of any
557 orientation (i.e. without considering orientation) of DNA motif sequences of
558 transcription factors, and (iii) EPA without being shortened by DNA motif sequences.
559 EPI predicted using the three types of EPA in common were removed. First, EPI
560 predicted based on EPA (i) were compared with chromatin interactions (Hi-C). The

561 resolution of chromatin interaction data used in this study was 50kb, so EPI were
562 adjusted to 50kb before their comparison. The number and ratio of EPI overlapped with
563 chromatin interactions were counted. Second, EPI were predicted based on EPA (ii), and
564 EPI predicted based on EPA (i) were removed from the EPI. The number and ratio of
565 EPI overlapped with chromatin interactions were counted. Third, EPI were predicted
566 based on EPA (iii), and EPI predicted based on EPA (i) and (ii) were removed from the
567 EPI. The number and ratio of EPI overlapped with chromatin interactions were counted.
568 The number and ratio of the EPI compared two times between EPA (i) and (iii), and
569 EPA (i) and (ii) (binomial distribution, $p$-value < 0.025 for each test).

570 For comparison of EPA with chromatin interactions (HiChIP) in $CD4^+$ T cells,
571 'GSM2705049_Naive_HiChIP_H3K27ac_B2T1_allValidPairs.txt' file was downloaded
572 from Gene Expression Omnibus (GEO) database (GSM2705049). The resolutions of
573 chromatin interaction data and EPI were adjusted to 1kb before their comparison.

574

575 **Acknowledgements**

576 The supercomputing resource was provided by Human Genome Center of the Institute
577 of Medical Science at the University of Tokyo. Computations were partially performed
578 on the NIG supercomputer at ROIS National Institute of Genetics. Publication charges
579 for this article were funded by JSPS KAKENHI Grant Number 16K00387. This
580 research was partially supported by the Platform Project for Supporting in Drug
581 Discovery and Life Science Research（Platform for Dynamic Approaches to Living
582 System）from Japan Agency for Medical Research and Development (AMED). This

research was partially supported by Development of Fundamental Technologies for Diagnosis and Therapy Based upon Epigenome Analysis from Japan Agency for Medical Research and Development (AMED). This work was partially supported by JST CREST Grant Number JPMJCR15G1, Japan.

## Figures

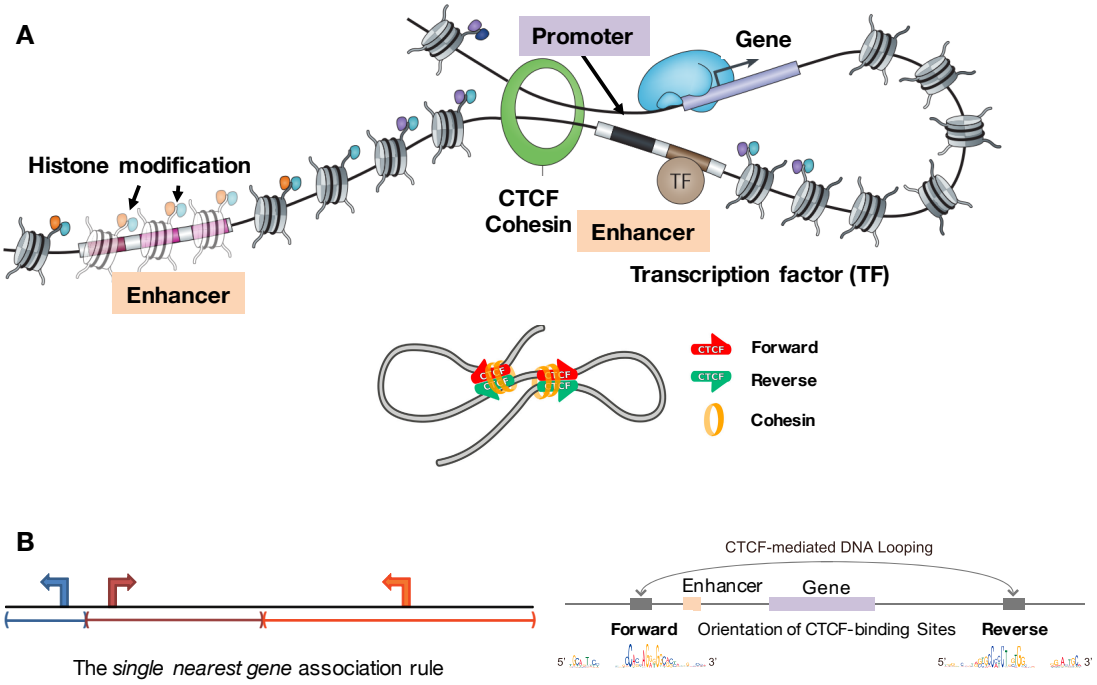


**Figure 1.** Chromatin interactions and enhancer-promoter association. (A) Forward–reverse orientation of CTCF-binding sites are frequently found in chromatin interaction anchors. CTCF can block the interaction between enhancers and promoters limiting the activity of enhancers to certain functional domains (de Wit et al. 2015; Guo et al. 2015). (B) Computationally-defined regulatory domains for enhancer-promoter association (McLean et al. 2010). The *single nearest gene* association rule extends the regulatory

597 domain to the midpoint between this gene's TSS and the nearest gene's TSS both
598 upstream and downstream. Enhancer-promoter association was shortened at the
599 genomic locations of forward-reverse orientation of DNA binding motif sequences of
600 transcription factors (e.g. CTCF in the figure).
601

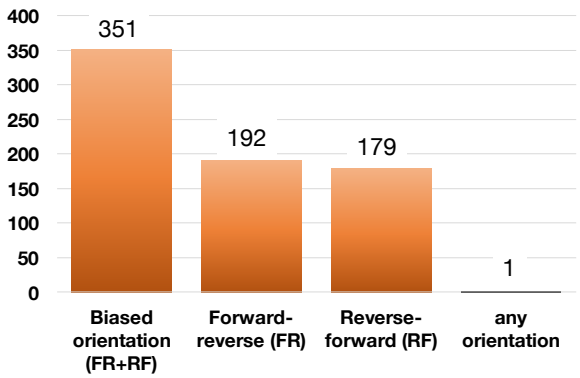


602

603 **Figure 2.** Biased-orientation of DNA motif sequences of transcription factors in
604 monocytes. Total 351 of biased orientation of DNA binding motif sequences of
605 transcription factors have been found to affect the expression level of putative
606 transcriptional target genes in monocytes of four people in common, whereas only one
607 any orientation (i.e. without considering orientation) of DNA binding motif sequences
608 have been found to affect the expression level.
609

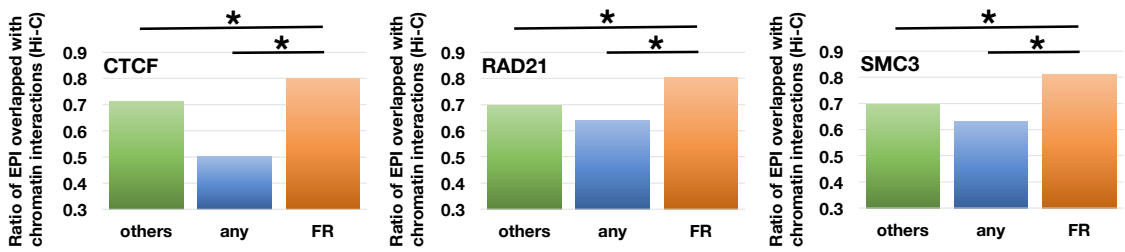


610

611 **Figure 3.** Comparison of DNA binding motif sequences of transcription factors with
612 chromatin interactions in monocytes. Total 62 biased orientation (41 FR and 24 RF) of
613 DNA motif sequences including CTCF and cohesin showed a higher ratio of EPI
614 overlapped with Hi-C than the other types of EPA in monocytes. FR: forward-reverse
615 orientation of DNA motifs. any: any orientation of DNA motifs. others:

enhancer-promoter association not shortened at the genomic locations of DNA motifs. * *p*-value < $10^{-5}$.

## Tables

**Table 1.** Top 90 biased orientation of DNA binding motif sequences of transcription factors in monocytes. TF: DNA binding motif sequences of transcription factors. Score: $-\log_{10}$ (*p*-value).

Forward-reverse orientation

| TF | Score | TF | Score | TF | Score |
|---|---|---|---|---|---|
| SRF | 136.39 | EBF | 55.63 | EGR2 | 37.31 |
| IRF7 | 119.13 | P53 | 54.99 | YLL054C | 37.20 |
| CLAMP | 107.65 | ZNF92 | 54.69 | ZNF316 | 37.15 |
| STAT1 | 105.40 | E47 | 52.16 | RSRFC4 | 36.96 |
| TFE3 | 94.78 | REST | 52.05 | PLAGL1 | 36.91 |
| ZNF623 | 90.72 | EIF5A2 | 51.51 | PACC | 36.76 |
| CEBPG | 90.30 | KLF14 | 51.36 | YBR033W | 36.32 |
| ZNF317 | 88.08 | TP63 | 50.43 | STA5A | 35.28 |
| ZNF93 | 87.64 | MAFA | 50.06 | TCF12 | 35.23 |
| SMAD2_SMAD3_SMAD4 | 85.65 | IKZF1 | 48.58 | RAD21 | 35.02 |
| ZNF836 | 81.83 | RDR1 | 48.04 | ZNF573 | 34.69 |
| E2F | 81.67 | SMC3 | 47.07 | EHF | 34.43 |
| FOXA1 | 75.73 | ESR2 | 47.03 | ZIC1 | 34.07 |
| MINI20 | 75.11 | YB1 | 46.87 | GCM1 | 34.00 |
| HMBOX1 | 72.11 | HIC1 | 46.40 | GLI2 | 33.53 |
| USF | 70.65 | NR1I2 | 46.29 | RXRA_VDR | 33.46 |
| ZNF660 | 68.80 | ZNF648 | 45.77 | GATA2 | 32.95 |
| STAT4 | 66.19 | ZN219 | 43.55 | TCFAP2C | 32.89 |
| HXB1 | 63.60 | HME1 | 43.47 | HNF4 | 32.83 |
| ZNF709 | 63.52 | NR2F6 | 42.34 | DEC | 32.83 |
| CTCF | 62.26 | ZNF33B | 41.81 | PF13 | 32.82 |
| FOXN2 | 61.95 | DREB2E | 41.72 | BTEB2 | 32.60 |
| D | 59.93 | NR2F2 | 41.24 | E2F8 | 32.38 |
| STA5B | 58.88 | ZNF214 | 41.22 | AT3G16280 | 31.88 |
| CMYB | 58.66 | CEBPZ | 40.56 | GLI1 | 31.75 |
| ZNF646 | 57.77 | ZNF695 | 39.37 | ZNF460 | 31.58 |
| MYB | 57.17 | AT3G04100 | 39.18 | GAL4P | 31.56 |
| ZNF716 | 56.47 | PTF1A | 38.20 | CPRF1 | 31.25 |
| ZNF676 | 56.30 | SMRC2 | 37.70 | STAT3 | 31.17 |
| KR | 55.78 | GCMA | 37.46 | WT1 | 31.03 |

633 Reverse-forward orientation

| TF | Score | TF | Score | TF | Score |
|---|---|---|---|---|---|
| RFX5 | 155.33 | NR2F1 | 54.18 | TCFAP2E | 42.44 |
| ZNF286B | 100.66 | ISL1 | 53.90 | BDP1 | 42.37 |
| ZNF225 | 97.70 | NFAC1 | 53.35 | AHR | 42.36 |
| CEBPB | 86.76 | RDS2 | 52.88 | TATA | 42.27 |
| SRF | 85.93 | NRF2 | 52.31 | ZNF449 | 42.05 |
| ZFP579 | 80.23 | RFX3 | 51.72 | SP8 | 41.63 |
| TCF1 | 79.47 | TCFAP2B | 51.52 | ZIC2 | 41.57 |
| SOX9 | 76.41 | ETV7 | 51.20 | ZFP202 | 41.27 |
| IRF3 | 75.35 | KLF16 | 50.51 | CRZ1P | 40.83 |
| ZNF28 | 71.26 | NFKB2 | 50.12 | VND | 40.72 |
| NFY | 69.96 | ZNF195 | 49.93 | ZNF652 | 40.55 |
| PAX5 | 69.88 | HAND1_E47 | 49.09 | CRZ1 | 40.18 |
| WT1 | 69.28 | ETV6 | 47.96 | MYOG | 39.93 |
| STAT1 | 69.06 | MAFK | 47.86 | ASCL2 | 39.92 |
| TOE3 | 68.44 | TBP | 47.63 | HSF2 | 39.69 |
| ZNF670 | 65.07 | NR5A2 | 47.55 | DOBOX5 | 39.39 |
| NANOG | 64.97 | LEU3 | 47.42 | SP3 | 38.95 |
| SP1 | 64.05 | SMAD3 | 47.22 | PO3F2 | 38.74 |
| TCF2 | 63.84 | ZNF331 | 46.93 | FLI1 | 38.72 |
| TEAD1 | 62.71 | ZNF238 | 46.86 | RXRA | 38.27 |
| NRF3 | 62.47 | ZSCAN2 | 46.77 | GABP1_GABP2 | 38.20 |
| NKX3 | 62.30 | CMYC_MAX | 45.48 | ZNF711 | 37.70 |
| ZBRK1 | 62.26 | HSF1 | 44.61 | SOX2 | 37.44 |
| STAT5B | 61.91 | ZBTB2 | 44.47 | RPH1 | 37.12 |
| CTCF | 60.90 | RAP1 | 44.47 | RBAK | 37.10 |
| PARP | 57.56 | CREM | 44.31 | ZN337 | 36.91 |
| STAT5A | 55.66 | ZNF343 | 44.03 | ZBTB7B | 36.73 |
| ZNF30 | 55.64 | ZBTB18 | 42.76 | ETV3 | 36.60 |
| E74A | 55.05 | OBOX2 | 42.53 | PO2F2 | 36.45 |
| ZNF687 | 54.64 | RNF96 | 42.48 | FOX | 36.01 |

634

635

636

637 **Table 2.** Top 30 forward-reverse orientation of DNA binding motif sequences of

638 transcription factors in MCF-7 and iPS cells. TF: DNA binding motif sequences of

639 transcription factors. Score: $-\log_{10}$ ($p$-value).

640 MCF-7 iPS

| TF | Score |
|---|---|
| CTCF | 43.69 |
| RAD21 | 27.00 |
| SMC3 | 26.64 |
| HOXA7 | 14.14 |
| E2F | 10.69 |
| CAC | 9.91 |
| DREB2E | 9.79 |
| BM9 | 9.67 |
| REST | 9.22 |
| STAT1 | 8.12 |
| SIRT6 | 8.03 |
| STA5B | 7.60 |
| KLF3 | 7.56 |
| PLAL1 | 6.88 |
| YY1 | 6.06 |
| CLAMP | 5.69 |
| RREB1 | 5.64 |
| ZN219 | 5.57 |
| PACC | 5.28 |
| SNT2 | 5.27 |
| ZBTB6 | 5.18 |
| MAZ | 4.77 |
| ZNF143 | 4.70 |
| E2F5 | 4.56 |
| ETS | 4.32 |
| STAT3 | 4.17 |
| KR | 3.70 |
| XRCC4 | 3.52 |
| SETB1 | 3.44 |
| DBP | 3.39 |

| TF | Score |
|---|---|
| STA5B | 34.45 |
| ZNF521 | 33.95 |
| E47 | 31.42 |
| E2F5 | 30.89 |
| ZBTB24 | 28.96 |
| CTCF | 26.94 |
| TFE3 | 26.55 |
| ZNF317 | 25.95 |
| ZNF143 | 24.73 |
| PAZ5 | 23.07 |
| BBX | 21.72 |
| HES1 | 21.17 |
| ZN148 | 21.13 |
| ZIC3 | 21.04 |
| STAT3 | 20.96 |
| STAT1 | 20.28 |
| AP1 | 20.09 |
| KLF3 | 18.15 |
| PARG | 17.78 |
| WT1 | 17.51 |
| XRCC4 | 17.08 |
| NKX25 | 16.99 |
| YLL054C | 16.85 |
| SIRT6 | 16.85 |
| MAZ | 16.46 |
| ETS | 15.72 |
| RUNX2 | 13.89 |
| SMC3 | 13.84 |
| RAD21 | 13.31 |
| EGR2 | 13.26 |

**Table 3.** Biased orientation of repeat DNA sequences in monocytes. Score: $-\log_{10}$ (*p*-value).

| Reverse-forward (RF) orientation | |
|---|---|
| DNA repeat seq. | Score |
| LTR16C | 81.65 |
| L1ME4b | 36.78 |
| AluSg | 32.26 |

**Table 4.** Top 30 of co-locations of biased orientation of DNA binding motif sequences of transcription factors in monocytes. Co-locations of DNA motif sequences of CTCF with other biased orientation of DNA motif sequences were shown in a separate table. Motif 1,2: DNA binding motif sequences of transcription factors. # both: the number of

653 open chromatin regions including both Motif 1 and Motif 2. # motif 1: the number of
654 open chromatin regions including Motif 1. # motif 2: the number of open chromatin
655 regions including Motif 2. # others: the number of open chromatin regions not including
656 Motif 1 or Motif 2. Open chromatin regions overlapped with histone modification
657 (H3K27ac) were used (Total 26,095 regions).

| Motif 1 | Motif 2 | # both | # motif 1 | # motif 2 | # others | *p*-value |
|---|---|---|---|---|---|---|
| CTCF | SMAD2 | 4527 | 781 | 4478 | 16309 | 0 |
| CTCF | RREB1 | 4379 | 929 | 4757 | 16030 | 0 |
| CTCF | ZN263 | 4357 | 951 | 4875 | 15912 | 0 |
| CTCF | SP1 | 4321 | 987 | 4052 | 16735 | 0 |
| CTCF | RAD21 | 3804 | 1504 | 225 | 20562 | 0 |
| CTCF | KLF6 | 3695 | 852 | 3800 | 17748 | 0 |
| CTCF | SMC3 | 1259 | 178 | 1977 | 22681 | 0 |
| CTCF | RXRA | 1220 | 259 | 2559 | 22057 | 0 |

658

| Motif 1 | Motif 2 | # both | # motif 1 | # motif 2 | # others | *p*-value |
|---|---|---|---|---|---|---|
| SMAD2 | ZN263 | 7427 | 1578 | 1805 | 15285 | 0 |
| SMRC2 | ZN263 | 7354 | 1192 | 1893 | 15656 | 0 |
| RREB1 | SP1 | 7208 | 1957 | 1165 | 15765 | 0 |
| SIRT6 | ZN263 | 7126 | 1154 | 2121 | 15694 | 0 |
| MAZ | SP1 | 7052 | 909 | 1321 | 16813 | 0 |
| MAZ | ZN263 | 7022 | 999 | 2225 | 15849 | 0 |
| SP1 | ZN263 | 7009 | 1364 | 2223 | 15499 | 0 |
| SMAD2 | SP1 | 6925 | 2080 | 1448 | 15642 | 0 |
| MAZ | RREB1 | 6920 | 967 | 2245 | 15963 | 0 |
| SIRT6 | SMAD2 | 6766 | 1514 | 2239 | 15576 | 0 |
| SIRT6 | SMRC2 | 6668 | 1612 | 1878 | 15937 | 0 |
| PLAL1 | SMAD2 | 6637 | 1074 | 2368 | 16016 | 0 |
| MAZ | SMAD2 | 6627 | 1334 | 2378 | 15756 | 0 |
| RARG | SMAD2 | 6602 | 1012 | 2403 | 16078 | 0 |
| PLAL1 | ZN263 | 6571 | 1140 | 2661 | 15723 | 0 |
| EGR2 | RREB1 | 6565 | 787 | 2600 | 16143 | 0 |
| KLF6 | RREB1 | 6563 | 932 | 2573 | 16027 | 0 |
| MAZ | SMRC2 | 6562 | 1459 | 1984 | 16090 | 0 |
| RREB1 | ZN263 | 6551 | 1607 | 2681 | 15256 | 0 |
| KLF6 | SP1 | 6541 | 954 | 1832 | 16768 | 0 |
| PLAL1 | RREB1 | 6496 | 1215 | 2640 | 15744 | 0 |
| EGR2 | SP1 | 6492 | 860 | 1881 | 16862 | 0 |
| KLF6 | SMAD2 | 6491 | 1004 | 2514 | 16086 | 0 |
| RARG | ZN263 | 6390 | 1224 | 2842 | 15639 | 0 |
| PLAL1 | SP1 | 6318 | 1393 | 2055 | 16329 | 0 |
| KLF6 | ZN263 | 6304 | 1191 | 2928 | 15672 | 0 |
| EGR2 | SMAD2 | 6270 | 1082 | 2735 | 16008 | 0 |
| EGR2 | ZN263 | 6253 | 1099 | 2979 | 15764 | 0 |
| RARG | RREB1 | 6219 | 1395 | 2917 | 15564 | 0 |
| EGR2 | MAZ | 6219 | 1133 | 1742 | 17001 | 0 |

659
660
661
662 **Table 5.** Comparison of biased orientation of DNA binding motif sequences of
663 transcription factors with chromatin interaction data in monocytes. TF: DNA binding

motif sequences of transcription factors. Score: $-\log_{10}$ ($p$-value). Score 1: Comparison of EPA shortened at genomic locations of FR or RF orientation of DNA binding sequences with EPA not shortened. Score 2: Comparison of EPA shortened at genomic locations of FR or RF orientation of DNA binding sequences with EPA shortened at genomic locations of any orientation of DNA binding sequences.

Forward-reverse

| TF | Score 1 | Score 2 |
|---|---|---|
| AP1 | 28.64 | 3.75 |
| AT3G04100 | 24.51 | 7.07 |
| BTEB2 | 8.64 | 2.69 |
| CTCF | 6.09 | 6.80 |
| E2F | 19.43 | 3.24 |
| E2F5 | 10.58 | 2.02 |
| EGR2 | 4.28 | 10.11 |
| ETS | 7.66 | 5.74 |
| FOSB | 7.98 | 1.99 |
| FOXO4 | 7.98 | 5.84 |
| GCM1 | 2.51 | 3.47 |
| GCR | 6.39 | 4.50 |
| IRF7 | 16.36 | 2.03 |
| KLF14 | 18.52 | 8.08 |
| KLF3 | 6.42 | 6.43 |
| MAZ | 1.82 | 4.55 |
| MIG2 | 42.64 | 6.22 |
| PARG | 5.38 | 4.21 |
| PITX3 | 10.31 | 5.62 |
| PLAL1 | 11.50 | 5.42 |
| PO6F1 | 31.28 | 7.60 |
| PTF1A | 8.91 | 4.50 |
| PU1 | 3.86 | 1.71 |
| RAD21 | 9.28 | 5.16 |
| RREB1 | 7.47 | 6.40 |
| RUNX2 | 2.97 | 1.68 |
| SETB1 | 1.63 | 2.08 |
| SMAD2 | 4.10 | 3.48 |
| SMC3 | 10.24 | 6.21 |
| SP1 | 20.98 | 4.64 |
| TCFAP2A | 5.10 | 1.63 |
| TF3B | 3.21 | 5.75 |
| TF3CB | 20.26 | 4.66 |
| TFE3 | 94.90 | 3.64 |
| YY1 | 13.88 | 7.04 |
| ZBTB6 | 15.08 | 3.93 |
| ZIC1 | 5.37 | 1.63 |
| ZN148 | 14.51 | 4.47 |
| ZN219 | 15.44 | 7.99 |
| ZNF28 | 11.88 | 3.36 |
| ZNF460 | 14.14 | 1.63 |

Reverse-forward orientation

| TF | Score 1 | Score 2 |
|---|---|---|
| ASCL2 | 6.23 | 3.80 |
| ATF3 | 17.21 | 2.23 |
| BC11A | 1.65 | 4.07 |
| BDP1 | 23.49 | 6.85 |
| CTCF | 12.32 | 11.74 |
| E2F2 | 23.33 | 1.95 |
| EBF1 | 14.83 | 7.11 |
| GABP1_GABP2 | 6.43 | 2.80 |
| IRF3 | 2.38 | 1.98 |
| IRF8 | 4.30 | 4.62 |
| NRF3 | 17.95 | 1.78 |
| PAX5 | 48.74 | 2.74 |
| POLR3A | 41.85 | 9.98 |
| RAD21 | 1.79 | 2.26 |
| RNF96 | 7.69 | 1.93 |
| RPN4 | 21.32 | 4.48 |
| RXRA | 29.89 | 11.87 |
| SMAD4 | 41.27 | 2.44 |
| SP2 | 2.09 | 11.15 |
| SP4 | 12.74 | 1.84 |
| SP8 | 20.03 | 2.17 |
| TCFAP2A | 8.90 | 3.53 |
| TCFAP2E | 5.72 | 1.84 |
| ZFP202 | 23.15 | 4.85 |

686 **References**

687

688 Bailey SD, Zhang X, Desai K, Aid M, Corradin O, Cowper-Sal Lari R, Akhtar-Zaidi B,
689 Scacheri PC, Haibe-Kains B, Lupien M. 2015. ZNF143 provides sequence
690 specificity to secure chromatin interactions at gene promoters. *Nat Commun* **2**:
691 6186.
692 Bailey TL, Boden M, Buske FA, Frith M, Grant CE, Clementi L, Ren J, Li WW, Noble
693 WS. 2009. MEME SUITE: tools for motif discovery and searching. *Nucleic*
694 *acids research* **37**: W202-208.
695 Barutcu AR, Lajoie BR, Fritz AJ, McCord RP, Nickerson JA, van Wijnen AJ, Lian JB,
696 Stein JL, Dekker J, Stein GS et al. 2016. SMARCA4 regulates gene expression
697 and higher-order chromatin structure in proliferating mammary epithelial cells.
698 *Genome research* **26**: 1188-1201.
699 Bejerano G, Lowe CB, Ahituv N, King B, Siepel A, Salama SR, Rubin EM, Kent WJ,
700 Haussler D. 2006. A distal enhancer and an ultraconserved exon are derived
701 from a novel retroposon. *Nature* **441**: 87-90.
702 de Souza FS, Franchini LF, Rubinstein M. 2013. Exaptation of transposable elements
703 into novel cis-regulatory elements: is the evidence always strong? *Mol Biol Evol*
704 **30**: 1239-1251.
705 de Wit E, Vos ES, Holwerda SJ, Valdes-Quezada C, Verstegen MJ, Teunissen H,
706 Splinter E, Wijchers PJ, Krijger PH, de Laat W. 2015. CTCF Binding Polarity
707 Determines Chromatin Looping. *Molecular cell* **60**: 676-684.
708 Grant CE, Bailey TL, Noble WS. 2011. FIMO: scanning for occurrences of a given
709 motif. *Bioinformatics (Oxford, England)* **27**: 1017-1018.
710 Guo Y, Xu Q, Canzio D, Shou J, Li J, Gorkin DU, Jung I, Wu H, Zhai Y, Tang Y et al.
711 2015. CRISPR Inversion of CTCF Sites Alters Genome Topology and
712 Enhancer/Promoter Function. *Cell* **162**: 900-910.
713 Javierre BM, Burren OS, Wilder SP, Kreuzhuber R, Hill SM, Sewitz S, Cairns J,
714 Wingett SW, Varnai C, Thiecke MJ et al. 2016. Lineage-Specific Genome
715 Architecture Links Enhancers and Non-coding Disease Variants to Target Gene
716 Promoters. *Cell* **167**: 1369-1384 e1319.
717 Jeong M, Huang X, Zhang X, Su J, Shamim M, Bochkov I, Reyes J, Jung H, Heikamp

718 E, Presser Aiden A et al. 2017. A Cell Type-Specific Class of Chromatin Loops
719 Anchored at Large DNA Methylation Nadirs. *bioRxiv*.
720 Ji X, Dadon DB, Abraham BJ, Lee TI, Jaenisch R, Bradner JE, Young RA. 2015.
721 Chromatin proteomic profiling reveals novel proteins associated with
722 histone-marked genomic regions. *Proc Natl Acad Sci U S A* **112**: 3841-3846.
723 Jin C, Kato K, Chimura T, Yamasaki T, Nakade K, Murata T, Li H, Pan J, Zhao M, Sun
724 K et al. 2006. Regulation of histone acetylation and nucleosome assembly by
725 transcription factor JDP2. *Nat Struct Mol Biol* **13**: 331-338.
726 Jjingo D, Conley AB, Wang J, Marino-Ramirez L, Lunyak VV, Jordan IK. 2014.
727 Mammalian-wide interspersed repeat (MIR)-derived enhancers and the
728 regulation of human gene expression. *Mob DNA* **5**: 14.
729 John S, Sabo PJ, Thurman RE, Sung MH, Biddie SC, Johnson TA, Hager GL,
730 Stamatoyannopoulos JA. 2011. Chromatin accessibility pre-determines
731 glucocorticoid receptor binding patterns. *Nature genetics* **43**: 264-268.
732 Jolma A, Yan J, Whitington T, Toivonen J, Nitta KR, Rastas P, Morgunova E, Enge M,
733 Taipale M, Wei G et al. 2013. DNA-binding specificities of human transcription
734 factors. *Cell* **152**: 327-339.
735 Karolchik D, Barber GP, Casper J, Clawson H, Cline MS, Diekhans M, Dreszer TR,
736 Fujita PA, Guruvadoo L, Haeussler M et al. 2014. The UCSC Genome Browser
737 database: 2014 update. *Nucleic acids research* **42**: D764-770.
738 Kheradpour P, Kellis M. 2014. Systematic discovery and characterization of regulatory
739 motifs in ENCODE TF binding experiments. *Nucleic acids research* **42**:
740 2976-2987.
741 Li H, Durbin R. 2009. Fast and accurate short read alignment with Burrows-Wheeler
742 transform. *Bioinformatics (Oxford, England)* **25**: 1754-1760.
743 Li H, Handsaker B, Wysoker A, Fennell T, Ruan J, Homer N, Marth G, Abecasis G,
744 Durbin R, Genome Project Data Processing S. 2009. The Sequence
745 Alignment/Map format and SAMtools. *Bioinformatics (Oxford, England)* **25**:
746 2078-2079.
747 McLean CY, Bristor D, Hiller M, Clarke SL, Schaar BT, Lowe CB, Wenger AM,
748 Bejerano G. 2010. GREAT improves functional interpretation of cis-regulatory
749 regions. *Nature biotechnology* **28**: 495-501.
750 Mumbach MR, Satpathy AT, Boyle EA, Dai C, Gowen BG, Cho SW, Nguyen ML,

751 Rubin AJ, Granja JM, Kazane KR et al. 2017. Enhancer connectome in primary
752 human cells identifies target genes of disease-associated DNA elements. *Nature*
753 *genetics* **49**: 1602-1612.
754 Newburger DE, Bulyk ML. 2009. UniPROBE: an online database of protein binding
755 microarray data on protein-DNA interactions. *Nucleic acids research* **37**:
756 D77-82.
757 Osato N. 2018. Characteristics of functional enrichment and gene expression level of
758 human putative transcriptional target genes. *BMC Genomics* **19**: 957.
759 Phanstiel DH, Van Bortle K, Spacek D, Hess GT, Shamim MS, Machol I, Love MI,
760 Aiden EL, Bassik MC, Snyder MP. 2017. Static and Dynamic DNA Loops form
761 AP-1-Bound Activation Hubs during Macrophage Development. *Molecular cell*
762 **67**: 1037-1048.e1036.
763 Portales-Casamar E, Thongjuea S, Kwon AT, Arenillas D, Zhao X, Valen E, Yusuf D,
764 Lenhard B, Wasserman WW, Sandelin A. 2010. JASPAR 2010: the greatly
765 expanded open-access database of transcription factor binding profiles. *Nucleic*
766 *acids research* **38**: D105-110.
767 Ramani V, Cusanovich DA, Hause RJ, Ma W, Qiu R, Deng X, Blau CA, Disteche CM,
768 Noble WS, Shendure J et al. 2016. Mapping 3D genome architecture through in
769 situ DNase Hi-C. *Nat Protoc* **11**: 2104-2121.
770 Rao SS, Huntley MH, Durand NC, Stamenova EK, Bochkov ID, Robinson JT, Sanborn
771 AL, Machol I, Omer AD, Lander ES et al. 2014. A 3D map of the human
772 genome at kilobase resolution reveals principles of chromatin looping. *Cell* **159**:
773 1665-1680.
774 Rebollo R, Romanish MT, Mager DL. 2012. Transposable elements: an abundant and
775 natural source of regulatory sequences for host genes. *Annu Rev Genet* **46**:
776 21-42.
777 Saeed S, Quintin J, Kerstens HH, Rao NA, Aghajanirefah A, Matarese F, Cheng SC,
778 Ratter J, Berentsen K, van der Ent MA et al. 2014. Epigenetic programming of
779 monocyte-to-macrophage differentiation and trained innate immunity. *Science*
780 *(New York, NY)* **345**: 1251086.
781 Schreiber J, Libbrecht M, Bilmes J, Noble W. 2017. Nucleotide sequence and DNaseI
782 sensitivity are predictive of 3D chromatin architecture. *bioRxiv*.
783 Tabuchi TM, Deplancke B, Osato N, Zhu LJ, Barrasa MI, Harrison MM, Horvitz HR,

784 Walhout AJ, Hagstrom KA. 2011. Chromosome-biased binding and gene
785 regulation by the Caenorhabditis elegans DRM complex. *PLoS Genet* **7**:
786 e1002074.
787 Wang J, Vicente-Garcia C, Seruggia D, Molto E, Fernandez-Minan A, Neto A, Lee E,
788 Gomez-Skarmeta JL, Montoliu L, Lunyak VV et al. 2015. MIR retrotransposon
789 sequences provide insulators to the human genome. *Proc Natl Acad Sci U S A*
790 **112**: E4428-4437.
791 Wang L, Wang S, Li W. 2012. RSeQC: quality control of RNA-seq experiments.
792 *Bioinformatics (Oxford, England)* **28**: 2184-2185.
793 Weintraub AS, Li CH, Zamudio AV, Sigova AA, Hannett NM, Day DS, Abraham BJ,
794 Cohen MA, Nabet B, Buckley DL et al. 2017. YY1 Is a Structural Regulator of
795 Enhancer-Promoter Loops. *Cell* **171**: 1573-1588 e1528.
796 Wingender E, Dietze P, Karas H, Knuppel R. 1996. TRANSFAC: a database on
797 transcription factors and their DNA binding sites. *Nucleic acids research* **24**:
798 238-241.
799 Xie Z, Hu S, Blackshaw S, Zhu H, Qian J. 2010. hPDI: a database of experimental
800 human protein-DNA interactions. *Bioinformatics (Oxford, England)* **26**:
801 287-289.
802 Zhang H, Li F, Jia Y, Xu B, Zhang Y, Li X, Zhang Z. 2017. Characteristic arrangement
803 of nucleosomes is predictive of chromatin interactions at kilobase resolution.
804 *Nucleic acids research* **45**: 12739-12751.
805 Zhang Y, An L, Xu J, Zhang B, Zheng WJ, Hu M, Tang J, Yue F. 2018. Enhancing Hi-C
806 data resolution with deep convolutional neural network HiCPlus. *Nat Commun*
807 **9**: 750.
808 Zhao Y, Stormo GD. 2011. Quantitative analysis demonstrates most transcription factors
809 require only simple models of specificity. *Nature biotechnology* **29**: 480-483.

810